

---

# Comparative Analysis of the Solar PV Power Plant Efficiency and Output Power at Navrongo in Ghana

Morrison Amenyio Vehe<sup>1</sup>, Joseph Cudjoe Attachie<sup>2,\*</sup>, Christian Kwaku Amuzuvi<sup>3</sup>

<sup>1</sup>Department of Electrical and Electronic Engineering, Regional Maritime University, Accra, Ghana

<sup>2</sup>Department of Electrical and Electronic Engineering, University of Mines and Technology, Tarkwa, Ghana

<sup>3</sup>Department of Renewable Energy Engineering, University of Mines and Technology, Tarkwa, Ghana

## Email address:

morrison.vehe@rmu.edu.gh (M. A. Vehe), jcattachie@umat.edu.gh (J. C. Attachie), ckamuzuvi@umat.edu.gh (C. K. Amuzuvi)

\*Corresponding author

## To cite this article:

Morrison Amenyio Vehe, Joseph Cudjoe Attachie, Christian Kwaku Amuzuvi. Comparative Analysis of the Solar PV Power Plant Efficiency and Output Power at Navrongo in Ghana. *Journal of Electrical and Electronic Engineering*. Vol. 10, No. 3, 2022, pp. 104-113.

doi: 10.11648/j.jeeec.20221003.15

**Received:** May 20, 2022; **Accepted:** June 8, 2022; **Published:** June 20, 2022

---

**Abstract:** In this paper, a comparative analysis of a 2.5 MW grid-connected solar photovoltaic (PV) power plant in Navrongo, Ghana is presented. The measured data from the plant was compared with that of the modelled and simulated results. The modelling was carried out using a genetic algorithm in MATLAB/Simulink. The comparison was based on power and solar irradiation as well as the efficiency of the plant under study. The results showed that, the model yielded increased output power compared with the power output determined from the measured data. This increase in power was observed in all three months; March, July and November 2014. PV module maximum power was more pronounced at a Fill Factor (FF) ranging from 0.5 to 0.8 at higher solar irradiation. Moreover, the efficiency of the modelled PV modules recorded a significant improvement in performance over that of the measured efficiencies for the same period. The monthly daily average measured efficiency value for March was 9.9% compared to 11.4% in the model, indicating a 1.5% increase. In July, however, efficiency increased by 1.0% by comparing the measured and modelled values of 9.6% and 10.6% respectively. November realised a 2.1% rise with a measured value of 11.2% against 13.3% being the modelled value. Conclusively, the study verifies the model's accuracy to a large extent.

**Keywords:** Photovoltaic, Comparative Analysis, Genetic Algorithms, Output Power, Efficiency

---

## 1. Introduction

With the rise in energy prices and the greenhouse effect, new energy-producing technologies such as fuel cells, biofuel cells, nuclear power, biomass, wind power, and photovoltaics are being vigorously developed. Photovoltaics (PV) appear to be the most promising of all these renewable sources. Indeed, only 0.2% of sun's energy that reaches the earth's surface is adequate to power the entire planet [1].

Ghana has relied to a large extent on hydro and thermal power to meet her energy demands in recent years. This means that, power outage in the country is a distinct possibility if the water levels drop or the gas supply from West Africa Gas and Ghana Gas Company is interrupted. Load shedding has been used as a last resort by the utility company to balance electricity supply and demand in Ghana on numerous occasions [2].

Presently, as a result of low energy production, there is a nationwide load shedding activity. A situation which hampers economic development and investor confidence even though, government is working hard to bring the situation under control.

Ghana has a total installed capacity of 2831 MW, with large hydro plants accounting for 55.8% of that capacity in April 2016 [3]. Volta River Authority (VRA) produces 75% of Ghana's power. [4]. In the near future, the government intends raising the capacity to 5,000 MW by incorporating renewable energy sources. As a result, the Renewable Energy Power (REP) Act 2011 was passed in December 2011 to establish a legislative framework for renewable energy development. Subsequently, VRA has taken a bold initiative of constructing a 2.5 MW grid-connected solar photovoltaic (PV) plant in Navrongo to supplement power generation from renewable energy sources [3].

BXC Company Ltd, a subsidiary of BXC Beijing China, followed VRA's strategic initiative and is currently operating a 20 MW solar PV power generating plant at Gomoa Onyadze in the Central Region of Ghana on test trial. A project, described as the largest solar PV farm in West Africa is capable of serving over 20000 homes with electricity when in full operation [5]. Mere Power Nzema Limited (MPNL), a private investor, is seeking Government Consent and Support Agreement (GCSA) to start its 155 MW grid connected solar PV plant project in Ghana's Western Region, which is expected to be followed by several more similar projects [6].

Fetyan and Hady, Esmailion et al., and Kymakis et al. published monitoring PV performance results to demonstrate the performance of system components, energy production, loss mechanisms associated with system operation, reliability and causes of system failures, validity of theoretical models using measured data, and long-term system performance [7-9].

The availability of solar radiation at a given place is vital to the success of any solar energy system, making precise understanding of solar resource data essential for planning and siting. Navrongo is a prominent market town in Ghana's Upper East Region, notable for its cathedral and grotto. It has a flat terrain and ecology that is typical of the sahel areas with solar intensity of 4 – 6.5 kWh/m<sup>2</sup>/day which is by far, the highest in Ghana making the area suitable for the solar PV power plant project [10]. The aim of this paper therefore, is to model and simulate the 2.5 MW grid-connected solar photovoltaic (PV) power plant and compare the results obtained with that of the measured data from the plant.

## 2. Materials and Methods

### 2.1. Energy Performance Modelling of Grid-Connected PV System

PV system performance modelling is mainly predicting the amount of solar radiation that will reach the surface of PV module with its temperature effect and then estimating the

instantaneous power, the module will generate. In the prediction process, variables are identified and their mathematical relationships with the PV system's power output established.

Field data were captured and analysed in Microsoft Excel due to its sufficient analytical tools required for this research work. Mathematical models were simulated in Matlab/Simulink programming environment. Matlab/Simulink is worldwide standard engineering software with wide range of applications in all engineering disciplines hence, used in this research.

### 2.2. Solar PV Cell Modelling

The power delivered by a solar PV module is dynamic since environmental and climate conditions keep changing hence, equivalent circuit parameters are considered important factors when analysing solar PV modules. To model and simulate solar PV module, the accuracy of the simulation is influenced by the equivalent circuit parameters. The equivalent circuit of a solar cell basically described by a current source parallel with a diode is termed as an ideal equivalent circuit [11].

According to Ma *et al.*, the elementary equation governing the behaviour of an ideal solar PV cell can be derived from the theory of semiconductors, which gives mathematical explanation to its I-V characteristic from equations 1 to 3 [12].

$$I = I_{ph} - I_d \quad (1)$$

$$I_d = I_o \left( \exp\left(\frac{qV}{AkT}\right) - 1 \right) \quad (2)$$

$$I = I_{ph} - I_o \left( \exp\left(\frac{qV}{AkT}\right) - 1 \right) \quad (3)$$

where I is the current produced by the solar cell (ampere),  $I_{ph}$  is the photo current (ampere),  $I_d$  is the diode current (ampere),  $I_o$  is the reverse saturation current (ampere), V is the voltage across the output terminals (volt), q is the elementary charge, A is diode ideality factor, k is the Boltzmann's constant, and T is the absolute temperature.

Figure 1 shows the I-V curve derived from equation (2).

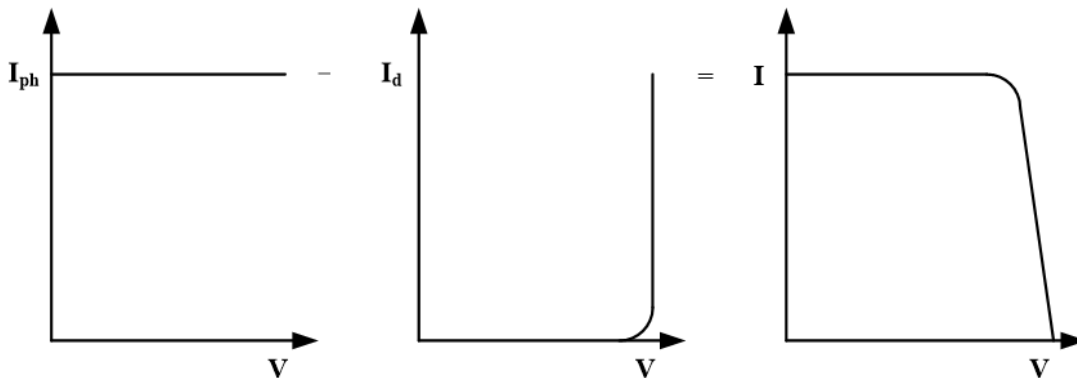


Figure 1. I-V Characteristics of an Ideal Model.

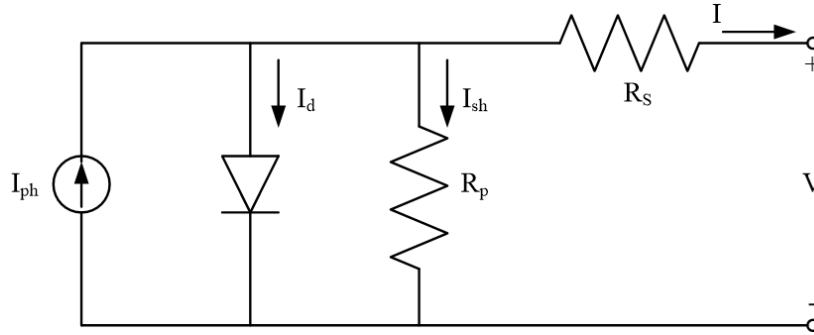


Figure 2. Equivalent Circuit of Single-Diode Model of a PV Cell.

**2.2.1. Single-Diode Model of a PV Cell**

The electrical equivalent circuit of single-diode model of a PV cell is shown in Figure 2. The resistances in the circuit are connected in series and parallel. This is because a practical PV array's I-V characteristic is not represented by a single cell. The equivalent circuit of a PV cell consists of a diode, a current source, a series resistance  $R_s$  and a parallel resistance  $R_p$ .

Several authors have advocated the single-diode model with  $R_p$  because of its precision [13]. The current source's photo current ( $I_{ph}$ ) is a function of incident sun irradiance and cell temperature. The P-N junction of a solar cell is represented by the diode. The diode saturation current ( $I_o$ ) is influenced by cell temperature and the diode ideality factor (A), both of which are taken into account in the equivalent circuit model. Voltage drop occurs at the exterior contacts of solar cells, which is expressed by series resistances  $R_s$  and  $R_p$ , which have higher influences in the voltage source and current source regions, respectively [14]. Leakage currents are represented by the parallel resistance  $R_p$ .

Based on Kirchoff's Current Law, equation (4) represents the extended version of the ideal model in equation (1). The I-V curve of a single-diode model with  $R_s$  and  $R_p$  in circuit is represented by the following equations as presented by Vimalarani and Kamaraj [11]:

$$I = I_{ph} - I_d - I_{sh} \tag{4}$$

where  $I_{sh}$  is the current flow through  $R_p$ .

The mathematical expressions for each of these currents are stated as follows:

$$I_{ph} = \frac{G}{G_{ref}} \times (I_{ph,ref} + \mu_{icc} \times (T - T_{ref})) \tag{5}$$

where  $G$  and  $T$  are the incident solar irradiance and cell temperature respectively,  $G_{ref} = 1000 \text{ W/m}^2$  and  $T_{ref} = 25^\circ\text{C}$  are incident solar irradiance and cell temperature respectively, at STCs,  $I_{ph,ref}$  is the current generated by the incident light at STCs, and  $\mu_{icc}$  is the temperature coefficient of the current.

The diode saturation current is given by:

$$I_d = I_o \left[ \exp \left( q \times \left( \frac{V + R_s I}{AkTN_s} \right) \right) - 1 \right] \tag{6}$$

The current flow ( $I_{sh}$ ) through shunt resistance  $R_p$  is given by:

$$I_{sh} = \frac{V + R_s I}{R_p} \tag{7}$$

From equations (6) and (7):

$$I = I_{ph} - I_o \times \left[ \exp \left( q \times \left( \frac{V + R_s I}{AkTN_s} \right) \right) - 1 \right] - \frac{V + R_s I}{R_p} \tag{8}$$

where  $N_s$  is the number of series connected cells in a module.

The PV module is made up of many cells connected in series and parallel to boost current and voltage, respectively. If the array is composed of  $N_p$  parallel connections of cells, the photo current and saturation currents may be expressed as  $I_{ph} = I_{ph,cell} N_p$  and  $I_o = I_{o,cell} N_p$ . In equation (8),  $R_s$  is the equivalent series resistance of the array and  $R_p$  is the equivalent parallel resistance.

**2.2.2. Two-Diode Model of a PV Cell**

The absence of recombination loss, which eventually leads to significant losses, makes the single-diode model unsuitable for modeling PV cells. Henceforth, an additional diode is added to the single-diode model and is subsequently referred to as the two-diode model [15].

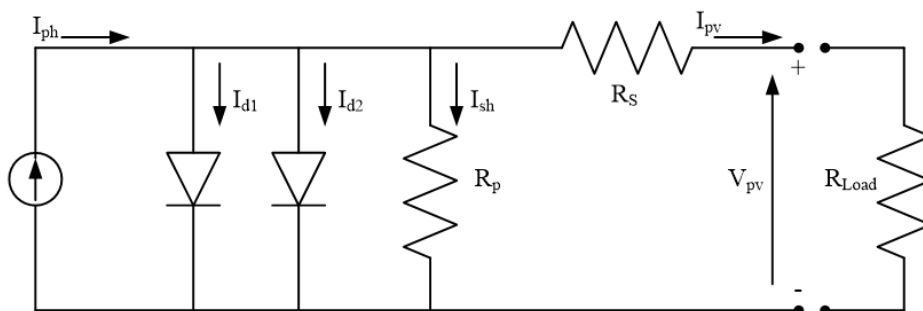


Figure 3. Equivalent Circuit of Two-Diode Model of a PV Cell.

As seen in Figure 3, the effect of carrier recombination is represented by the second diode in a two-diode model. The two-diode model is employed in this research work because the characteristics of the equivalent circuit utilised will improve the solar PV model's accuracy.

By applying Kirchoff's current law to Figure 3, the module output current (I) can be represented as:

$$I_{pv} = I_{ph} - I_{d1} - I_{d2} - I_{sh} \quad (9)$$

The respective expressions of  $I_{d1}$  and  $I_{d2}$  as presented by Ishaque *et al.* when substituted into equation (9) results in:

$$I_{pv} = I_{ph} - I_{o1} \left[ \exp \left( \frac{V + IR_s}{A_1 V T_1} \right) - 1 \right] - I_{o2} \left[ \exp \left( \frac{V + IR_s}{A_2 V T_2} \right) - 1 \right] - \left( \frac{V + IR_s}{R_p} \right) \quad (10)$$

where  $I_{o1}$  and  $I_{o2}$  are reverse saturation currents for diode 1 and 2 respectively;  $I_{o2}$  represents the recombination loss in the depletion region [14],  $V_{T1,2} = N_s k T / q$  is the thermal voltage of the solar PV module,  $N_s$  is the number of series connected cells,  $A_1$  and  $A_2$  correspond to diode ideality factors for diode 1 and 2 respectively.  $A_1$  and  $A_2$  represent the diffusion and recombination current respectively [16, 14].

PV modules manufacturers provide some few experimental data on electrical and thermal properties of the module in the manufacturer's datasheet but neglect some equally relevant parameters required to comprehensively model the PV module.

The datasheet does not capture parameters such as photocurrent, series and shunt resistances, diode ideality factor and reverse saturation current, as well as the bandgap energy of the semiconductor.

Generators are categorised as either current or voltage sources. Therefore, depending on the operating point, practical PV devices exhibit hybrid behavior, which can be either a current or voltage source. In practice, PV devices have a series resistance  $R_s$  whose influence is stronger when the devices operate in the voltage source region and a parallel resistance  $R_p$  with stronger influence in the current source region of operation. Since series resistance is low and the parallel resistance is high in practical PV devices, it is mostly assumed that,  $I_{sc} \approx I_{pv}$  and is used in the modelling of PV modules [14].

### 2.3. The PV Modules Datasheet

Two different PV modules manufactured by SunTech and Jinko Solar Companies are installed at the study site. Their relevant specifications for modeling in this research are captured in Table 1.

### 2.4. The PV Modules Datasheet

In order to validate the PV modules, the various equations to determine the output current, voltage and power were implemented in Simulink blocks.

**Table 1.** Design Specification of SunTech and JinKo PV Modules.

SN	Parameters	SunTech PV Module	JinKo PV Module
1	Optimum Operating Voltage ( $V_{mp}$ )	35.7 V	36.2 V
2	Optimum Operating Current ( $I_{mp}$ )	8.27 A	8.15 A
3	Open Circuit Voltage ( $V_{oc}$ )	45.1 V	45.1 V
4	Short Circuit Current ( $I_{sc}$ )	8.57 A	8.76 A
5	Maximum Power at STC ( $P_{max}$ )	295 W	295 W
6	Maximum Power at NOCT ( $P_{max}$ )	215 W	218 W
7	Module Efficiency at STC	15.2%	15.2%
8	Number of Cells	72	72
9	Nominal Operating Cell Temperature (NOCT)	42.2	42.2
10	Operating Module Temperature	-40°C to +85°C	
11	Temperature Coefficient of $P_{max}$	-0.44 %/°C	-0.44 %/°C
12	Temperature Coefficient of $V_{oc}$	-0.33 %/°C	-0.33 %/°C
13	Temperature Coefficient of $I_{sc}$	0.55 %/°C	0.06 %/°C

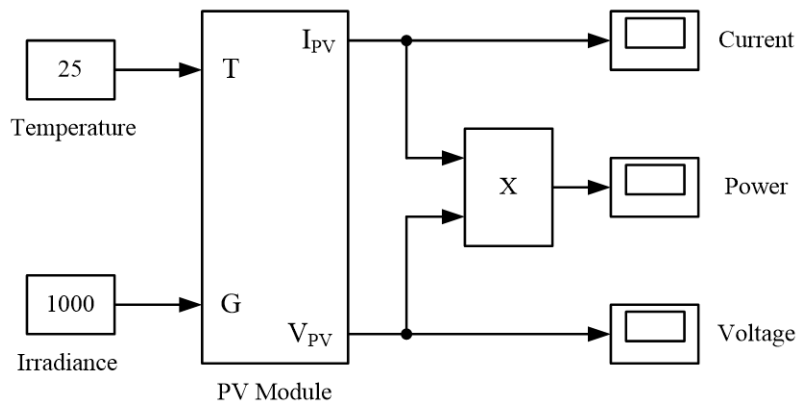


**Figure 4.** The PV Model Simulator Block Representation in Simulink.

In summary, Figure 4 represents a model of the whole PV Simulator block in Simulink.

**2.5. Energy Output Modelling of PV System**

PV system energy output modelling involves identifying all independent variables and establishing their mathematical relationships with power output. The variables identified from literature for the purpose of this research includes: solar radiation; ambient temperature, module temperature, module efficiency, module area and wind speed.

**2.6. Genetic Algorithm**

Genetic algorithm (GA) is a method used in solving both constrained and unconstrained optimisation problems inspired by Darwin’s theory of evolution, which employs the “survival of the fittest” concept of natural biological evolution. GA repeatedly modifies a population of individual solutions and at each step; individuals are selected at random from a prevailing population to be parents which are subsequently used to produce the children for the next generation. Over successive generations, the population “evolves” toward an optimal solution.

In GA, three main types of rules are used at each step to create the next generation from the present population:

- i). Selection rules select the individuals, called parents, which contribute to the population at the next generation;
- ii). Crossover rules combine two parents to form children for the next generation; and
- iii). Mutation rules apply random changes to individual parents to form children.

GA can be applied in solving a number of optimisation problems that are not suitable for standard optimisation algorithms. These include problems in which the objective function is discontinuous, non-differentiable, stochastic, or highly nonlinear problems [17].

**2.7. The Optimisation Problem**

The objective function for the optimisation problem is formulated from the concept of deriving maximum power from a PV module based on its Fill Factor (FF). This FF describes the characteristics of a PV array hence, a key parameter in evaluating its operating performance. As presented by Guda & Aliyu, equation (11) describes the fill factor [18]:

$$FF = \frac{V_{mp} I_{mp}}{V_{oc1} I_{sc1}} \tag{11}$$

The short circuit current  $I_{sc1}$  is a function of solar irradiance and the PV module temperature and is given as:

$$I_{sc1} = I_{sco} \times [1 + \alpha(T_1 - T_0)] \times (G_1/G_o) \tag{12}$$

where  $I_{sco}$  is the short circuit current of the PV module and  $G_o$ , solar irradiance at STC.  $G_1$  is the solar irradiance due to changes in the environment,  $I_{sc1}$  is the short circuit current and  $\alpha$  is the PV module’s electrical specification.

The open circuit voltage ( $V_{oc1}$ ) is also given as:

$$V_{oc1} = V_{oc0} \times [1 + \beta(T_1 - T_0)] \tag{13}$$

where  $V_{oc0}$  is the open circuit voltage under STC.

The maximum power point on the I-V curve of a PV module occurs at the “knee” of the curve. Since the FF determines the power output of the PV module, the maximum power output is given by the relation:

$$P_{max} = FF \times V_{oc} \times I_{sc} \tag{14}$$

The PV system which is made of a collection of PV modules connected in series and parallel to derive the respective required voltage and current is considered as a matrix of  $M_s \times M_p$  PV modules. The voltage and current scaling are therefore, given as follows:

$$I_A = M_p \times I_M \tag{15}$$

$$V_A = M_s \times V_M \tag{16}$$

where  $I_A$  and  $V_A$  are the PV array current and voltage respectively;  $I_M$  and  $V_M$  are the PV module current and voltage.

From equations (11) to (16), the maximum power output of the PV array can be expressed as:

$$P_A = FF_A \times V_A \times I_A = M_p \times M_s \times P_M \tag{17}$$

where  $P_A$  and  $P_M$  are the respective PV array and module power output.

Figure 5 is the structure of the proposed GA based PV system power output implementation where  $P_{out}$  is the output power.

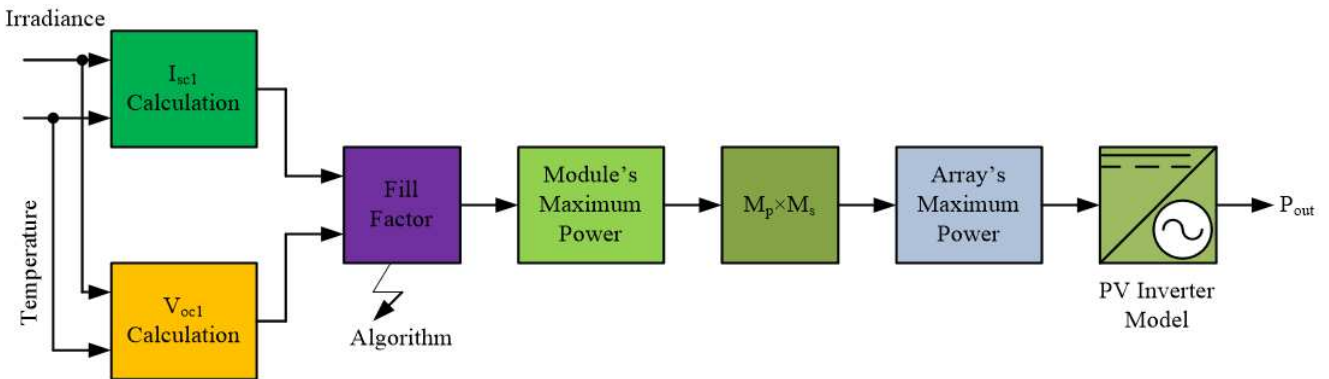


Figure 5. Structure of GA Based PV System Power Output.

The proposed GA procedure is implemented as follows: Initial Population, Fitness Evaluation, and Genetic Operators. The above conditions are elucidated in [19]. A general procedure followed to implement GA in this research work is shown in Figure 6.

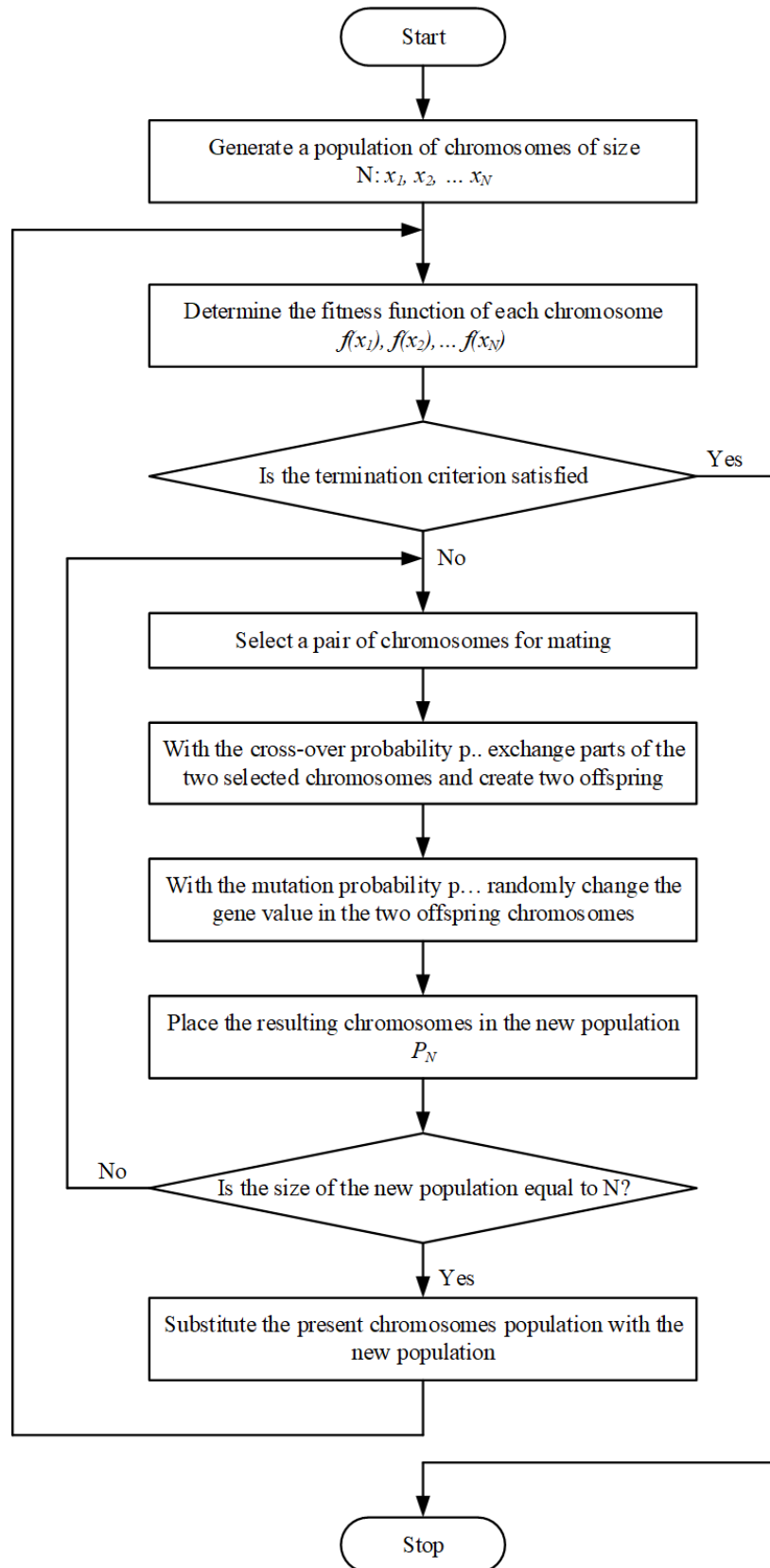


Figure 6. Generic GA Flow Chart for the Optimisation.

### 3. Results and Discussions

#### 3.1. Simulation Results

The simulation results are hereby presented from Figures 7 to 16.

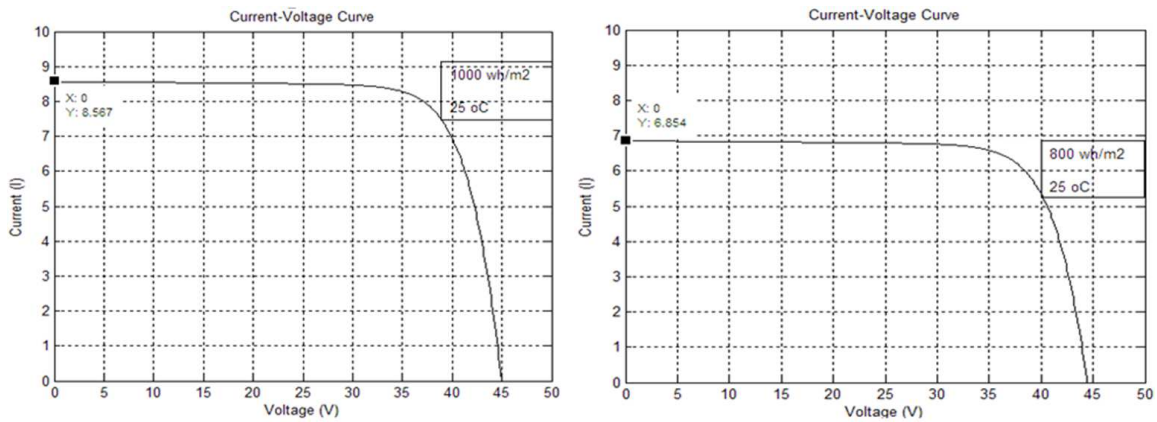


Figure 7. I-V Curves of Modelled SunTech PV Module at Difference Irradiation.

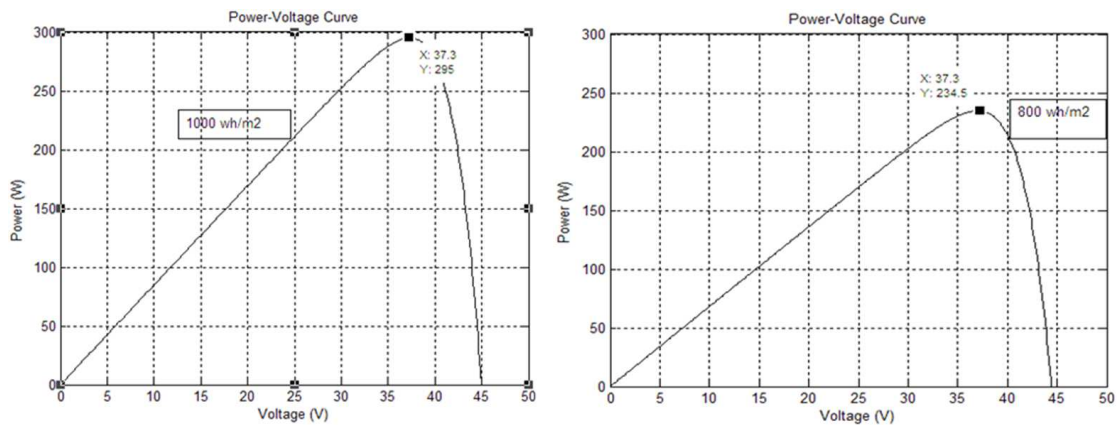


Figure 8. P-V Curves of Modelled SunTech PV Module at Difference Irradiation.

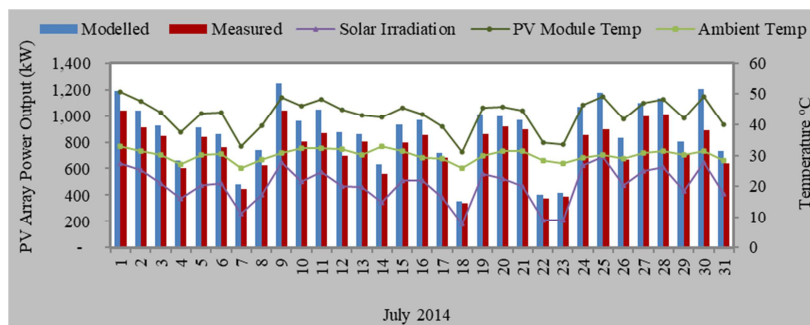


Figure 9. PV Array Modelled and Measured Power Output, Solar Irradiation, Ambient and Module Temperature.

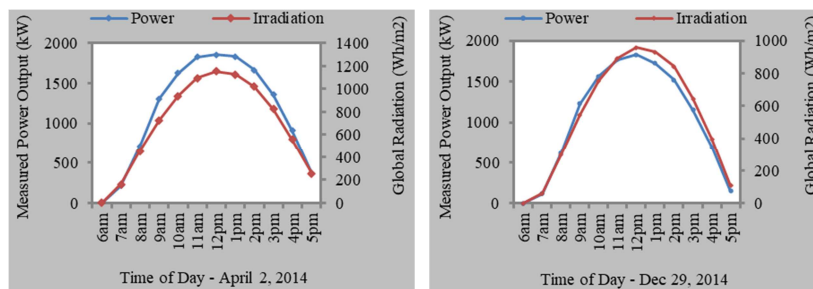


Figure 10. PV Array Daily Measured Power Output and Solar Irradiation for April and December.

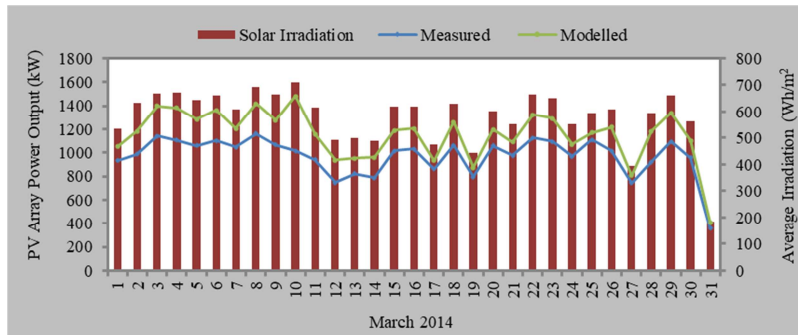


Figure 11. PV Array Measured, Modelled Power Output and Solar Irradiation.

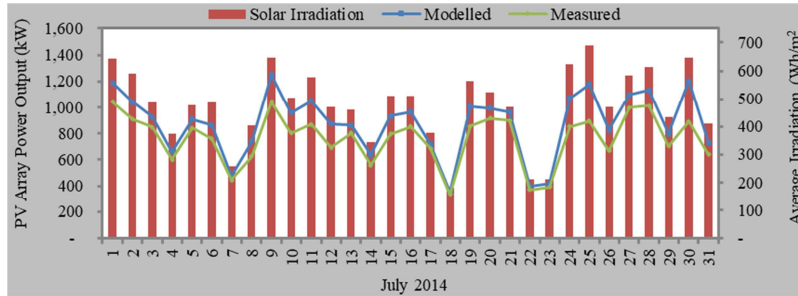


Figure 12. PV Array Measured and Modelled Power Output and Solar Irradiation.

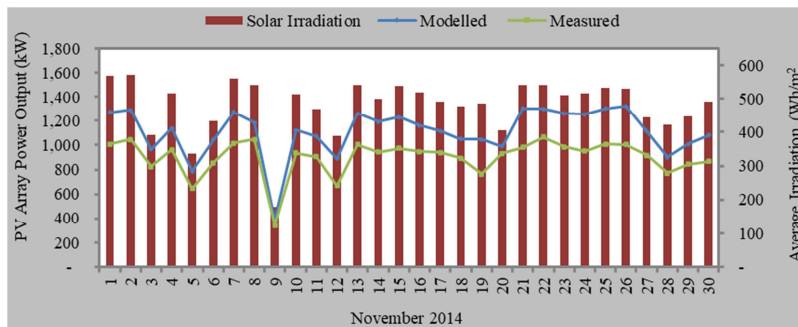


Figure 13. PV Array Measured and Modelled Power Output and Solar Irradiation.

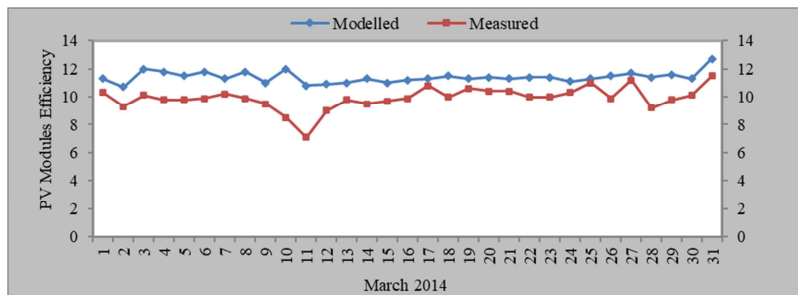


Figure 14. PV Array Measured and Modelled Efficiencies.

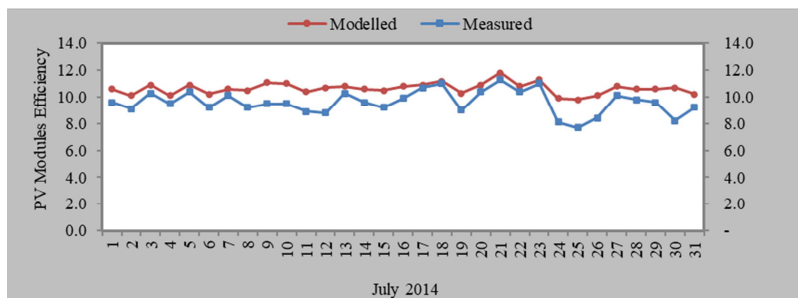


Figure 15. PV Array Measured and Modelled Efficiencies.

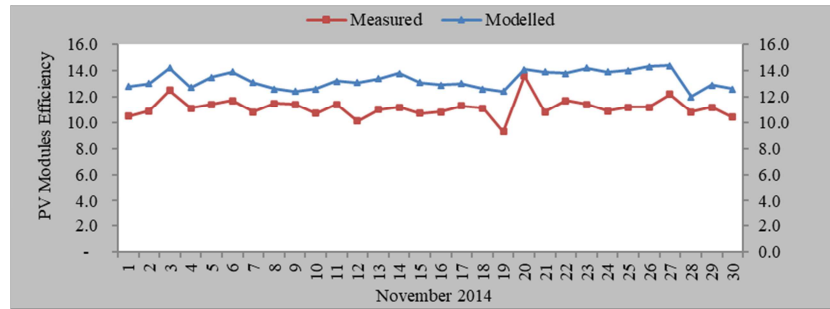


Figure 16. PV Array Measured and Modelled Efficiencies.

## 3.2. Discussions

### 3.2.1. PV Array Power Output and Solar Irradiation

The PV array output power is largely influenced by the solar radiation rather than the module and the ambient temperature. This is revealed in Figure 9 where the irradiation positively correlates the power output, and it is more evident in Figure 10. On the other hand, both ambient and PV module temperatures increase alongside the output power. According to the PV modules datasheet in Table 1, the modules are seen on the average, to be operating in an acceptable and favourable temperature condition. It can be seen that; the level of temperature rise does not negatively affect the output power.

### 3.2.2. PV Array Measured and Modelled Output Power and Solar Irradiation

As revealed in Figures 11, 12, and 13 the model yielded increased output power compared with the power output determined from the measured data. This increase in power is observed in all three months; March, July and November, 2014 arbitrary chosen. PV module maximum power is more pronounced at Fill Factor (FF) ranging from 0.5 to 0.8 at higher solar irradiation.

### 3.2.3. PV Modules Measured and Modelled Efficiency

The modelled PV modules efficiency recorded a substantial improvement in performance over the measured efficiency for the arbitrary chosen months of March, July and November 2014 as presented in Figures 14 to 16. The monthly daily average measured efficiency value for March was 9.9% against modelled value of 11.4% and this chalked an increase of 1.5%. July on the other hand noted 1.0% rise in efficiency with measured value of 9.6% and 10.6% as modelled. November realised 2.1% improvement with a measured value of 11.2% against 13.3% as the modelled value.

## 4. Conclusions

A comparative study on the 2.5 MW peak grid-connected solar photovoltaic power plant installed at Navrongo was estimated based on a monthly average for 1-year, and subsequently modelled using a Genetic Algorithm in MATLAB/Simulink. The following conclusions were drawn from the study:

- i). The PV modules output power is largely influenced by

the solar irradiation rather than the ambient and module temperatures;

- ii). The model yielded increased output power compared with the power output determined from the measured data. Moreso, PV module output power increases at higher fill factor, thus ranging from 0.5 to 0.8 at higher solar irradiation; and
- iii). The modelled PV modules efficiency recorded a significant improvement in performance over the measured efficiencies for March, July and November 2014.

## 5. Recommendations

The following recommendations are provided:

- i). Accumulation of dust on PV modules surface can significantly reduce the output power due to inefficient use of solar irradiation. Effective and efficient cleaning of PV modules surface is therefore recommended in the solar PV power plant's operation and maintenance at Navrongo to practically realised the improved efficiency; and
- ii). Future work should consider the tilt angle of the mounted PV modules to ascertain it is at the appropriate angle to deliver optimum energy.

## References

- [1] Attachie, J. C. and Amuzuvi, C. K. (2013), "Renewable Energy Technologies in Ghana: Opportunities and Threats", *Research Journal of Applied Sciences, Engineering and Technology*, Vol. 6, No. 5, pp. 776-782.
- [2] Mahama, E. K. (2013), "Renewable Energy: An Alternative to Meeting Ghana's Energy Challenges", [www.vibeghana.com/2013/04/08/renewable-energy-an-alternative-to-meeting-ghanas-energy-challenges/](http://www.vibeghana.com/2013/04/08/renewable-energy-an-alternative-to-meeting-ghanas-energy-challenges/), Accessed: October 6, 2015.
- [3] Anon. (2016), "Power Generation Facts and Figures", [www.vraghana.com/resources/facts.php](http://www.vraghana.com/resources/facts.php), Accessed: April 13, 2016.
- [4] Yatey, E. (2015), "Ghana's Road to Energy Sufficiency", [www.africanreview.com](http://www.africanreview.com). Accessed: February 3, 2015.
- [5] Kale-Dery, S. (2015), "Solar Power Generating Plant on Test Trial", [www.graphic.com.gh/news/general-news/53683-solar-power-generating-plant-on-test-trial.html](http://www.graphic.com.gh/news/general-news/53683-solar-power-generating-plant-on-test-trial.html), Accessed: April 13, 2016.

- [6] Acheampong, J. (2014), "US\$350 Million Solar Project for Ghana", [www.graphic.com.gh/business/business-news/18704-us-350-million-solar-project-for-ghana.html#sthash.EGPK7UVR.dpuf](http://www.graphic.com.gh/business/business-news/18704-us-350-million-solar-project-for-ghana.html#sthash.EGPK7UVR.dpuf), Accessed: April 13, 2016.
- [7] Fetyan, K. M. and Hady, R. (2021), "Performance Evaluation of on-grid PV Systems in Egypt", *Water Science*, 35: 1, 63-70, DOI: 10.1080/23570008.2021.1905347.
- [8] Esmailion, F., Ahmadi, A., Esmailion, A. and Alihyaei, M. (2021), "The Performance Analysis and Monitoring of Grid-Connected Photovoltaic Power Plant", *Current Chinese Computer Science*, Volume 1, Issue 1, doi: 10.2174/2665997201999200511083228.
- [9] Kymakis, E., Kalykakis, S. and Papazoglou, T. M. (2009), "Performance Analysis of a Grid-Connected Photovoltaic Park on the Island of Crete", *Energy Conversion and Management*, Vol. 50, No. 3, pp. 433-438.
- [10] Omane, F. (2013), "Status and Development of the Local PV Market Structure", [www.giz.de/fachexpertise/downloads/2013-en-pep-informationsveranstaltung-pv-ghana-frimpong.pdf](http://www.giz.de/fachexpertise/downloads/2013-en-pep-informationsveranstaltung-pv-ghana-frimpong.pdf), Accessed: September 4, 2015.
- [11] Vimalarani, C. and Kamaraj, N. (2015), "Modeling and Performance Analysis of the Solar Photovoltaic Cell Model Using Embedded Matlab", *Transactions of the Society for Modeling and Simulation International*, 16pp.
- [12] Ma, T., Yang, H. and Lu, L. (2014), "Photovoltaic System Modeling and Performance Prediction", *Renewable Sustainable Energy Rev*, Vol. 36, pp. 304-315.
- [13] Ishaque, K., Salam, Z. and Syafaruddin (2011), "A Comprehensive Matlab Simulink PV System Simulator with Partial Shading Capability Based on Two-Diode Model", *Solar Energy*, Vol. 85, pp. 2217-2227.
- [14] Villalva, M. G., Gazoli, J. R. and Filho, E. R. (2009), "Comprehensive Approach to Modeling and Simulation of Photovoltaic Arrays", *IEEE Transactions on Power Electronics*, Vol. 24, No. 5, pp. 1198-1208.
- [15] Ishaque, K. Salam, Z. and Taheri, H. (2011a), "Simple, Fast and Accurate Two-Diode Model for Photovoltaic Modules", *Solar Energy Materials Solar Cells*, Vol. 95, No. 2, pp. 586-594.
- [16] Ishaque, K., Salam, Z. and Taheri, H. (2011b), "Accurate Matlab Simulink PV System Simulator Based on a Two-Diode Model", *Journal of Power Electronics*, Vol. 11, No. 2, pp. 179-187.
- [17] Anon. (2014e), "Global Optimization Toolbox User's Guide for MATLAB (R2014a)", Mathworks, 2014.
- [18] Guda, H. A. and Aliyu U. O. (2015), "Effects of Temperature on Photovoltaic Array Conversion Efficiency and Fill Factor", *International Journal of Engineering and Technology*, Vol. 5, No. 1, 7 pp.
- [19] Sivanandam, S. N. and Deeper, S. N. (2008), *Introduction to Genetic Algorithms*, Springer, New York, 453pp.